JACS
JOURNAL OF THE AMERICAN CHEMICAL SOCIETY
Communication
pubs.acs.org/JACS

Redox-Controlled Selective Docking in a [2]Catenane Host

Gokhan Barin,[†,⊥,‡] Marco Frasconi,[†,‡] Scott M. Dyar,[†,§] Julien Iehl,[†] Onur Buyukcakir,[†] Amy A. Sarjeant,[†] Raanan Carmieli,[†,§] Ali Coskun,[†,⊥] Michael R. Wasielewski,[†,§] and J. Fraser Stoddart*[,†,⊥]

[†]Department of Chemistry and [§]Argonne−Northwestern Solar Energy Research (ANSER) Center, Northwestern University, Evanston, Illinois 60208, United States

[⊥]Department of Chemistry and Graduate School of EEWS, Korea Advanced Institute of Science and Technology (KAIST), Daejeon 305-701, Republic of Korea

Ⓢ *Supporting Information*

ABSTRACT: The docking by neutral and charged guests selectively in two geometrically different binding pockets in a dynamic [2]catenane host is demonstrated in the solid state by manipulating its redox chemistry. The change in redox properties, not only alters the affinity of the host toward neutral and charged guests, but it also induces a profound change in the geometry of the host to accommodate them. X-ray crystallography, performed on the two different 1:1 complexes, demonstrates unambiguously the fact that the [2]catenane host provides a uniquely different binding pocket wherein a methyl viologen dication is stabilized by interacting with a bipyridinium radical cation, despite the presence of Coulombic repulsions.

For some time now, mechanically interlocked molecules[1] (MIMs)—particularly catenanes and rotaxanes—have been synthesized in good yields employing template-directed protocols.[2] The efficiency of these protocols relies mainly on the strength of the noncovalent bonding interactions between the components. In the context of donor−acceptor systems, the tetracationic cyclophane, cyclobis(paraquat-*p*-phenylene) ($CBPQT^{4+}$), has been one of the most widely investigated rings when employing templates to make[3] MIMs. More recently, we have demonstrated[4] that the $CBPQT^{4+}$ ring is also a powerful building block for the construction of MIMs when harnessing radical−radical interactions as the source of templation. The discovery that the $CBPQT^{4+}$ ring can form[4a,5] a strong complex ($\mathbf{MV}^{\bullet+}\subset CBPQT^{2(\bullet+)}$) with methyl viologen ($\mathbf{MV}^{2+}$) under reductive conditions, has not only led[4b] to the preparation of otherwise difficult to make MIMs, but it has also enabled[6] the investigation of their switching mechanisms based on radical-pairing interactions which provide a valuable additional handle to control the properties of (bistable) MIMs both in solution and in the solid state.[7]

Scheme 1. Structural Representations of the [2]Catenane $\mathbf{C}^{4+}$ and the Equilibration between Two Possible Co-conformations (States I and II) Associated with Translational Motion of the TTF Unit in the Macrocyclic Polyether, Resulting in the Formation of Two Different Binding Pockets (Light Brown Parallelograms)[a]

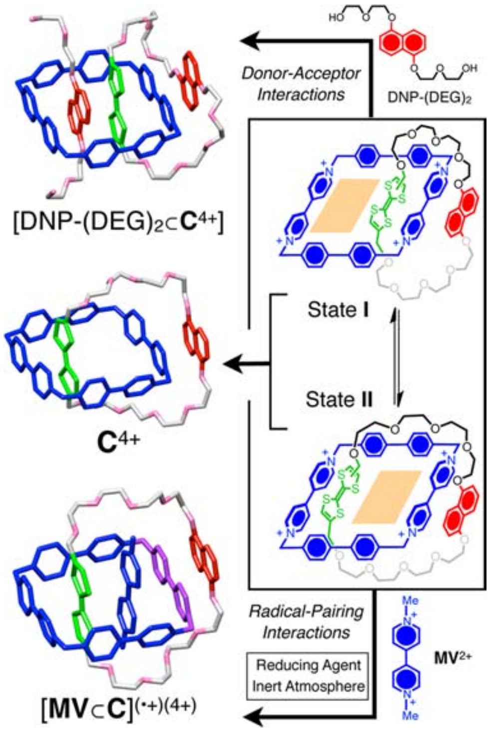

[a]$\mathbf{C}^{4+}$ exists[8] in state **II** in its solid state, as indicated by tubular representation of its X-ray crystal structure. Similar representations show the solid-state superstructures of [(DNP-(DEG)$_2$$\subset\mathbf{C}^{4+}$] and [$(\mathbf{MV}\subset\mathbf{C})^{(\bullet+)(4+)}$] obtained by docking DNP-(DEG)$_2$ and $\mathbf{MV}^{2+}$, respectively, in the different binding pockets using donor−acceptor and radical-pairing recognition.

Recently, we reported[8] the synthesis of the [2]catenane $\mathbf{C}\cdot 4PF_6$ (Scheme 1) as the precursor to self-assembling a *rotacatenane*[9] by a "threading-followed-by-stoppering" approach upon formation of a complex between $\mathbf{C}^{4+}$ and substrates incorporating *π*-electron-rich recognition sites, namely, tetrathiafulvalene (TTF) and 1,5-dioxynaphthalene (DNP). $\mathbf{C}^{4+}$ can be employed as a host—owing to the large cavity size of the tetracationic molecular square ($\mathbf{MS}^{4+}$), cyclobis(paraquat-4,4′-biphenylene)—to obtain even more sophisticated MIMs, e.g., a [3]rotacatenane.[10] The macrocyclic polyether component of $\mathbf{C}^{4+}$ has the freedom to move within the MS^{4+} component in

Received: December 21, 2012
Published: January 25, 2013

dx.doi.org/10.1021/ja3125004 | *J. Am. Chem. Soc.* 2013, 135, 2466−2469

solution, resulting in a shift in the position of the binding site between states **I** and **II** (Scheme 1). In fact, this dichotomy is expressed[8] in the solid-state structure of $\mathbf{C}^{4+}$ in which the TTF unit interacts with the alongside bipyridinium dication (BIPY^{2+}), i.e., the [2]catenane exists in state **II**. Upon addition, however, of the diethyleneglycol (DEG)-substituted DNP derivative DNP-$(\mathrm{DEG})_2$, the cavity of $\mathbf{C}^{4+}$ in state **I** is occupied preferentially as revealed by its X-ray crystal structure. This observation has led us to investigate whether it is possible to form host–guest complexes in which the guest occupies the cavity of $\mathbf{C}^{4+}$ in state **II**. We envisage that developing a strategy to control the stereochemical outcome of such an association has the potential to uncover new molecular topologies. Herein, we report a strategy for the selective docking of the two different binding pockets (states **I** and **II**) of $\mathbf{C}^{4+}$ in the solid state as a result of donor–acceptor and radical-pairing interactions. The solid-state structure of the [3]pseudorotacatenane, which is obtained from a mixture of $\mathbf{C}^{4+}$ and $\mathbf{MV}^{2+}$ under reductive conditions, reveals the docking of the guest $\mathbf{MV}^{2+}$ in the binding pocket of the monoreduced [2]catenane ($\mathbf{C}^{(\bullet+)(2+)}$) when it is in state **II** and has also led to the observation of the ($\mathrm{BIPY}^{2+}\cdots\mathrm{BIPY}^{\bullet+}$) interaction in a confined environment in the solid state.

First, we investigated the interaction between $\mathbf{C}^{2(\bullet+)}$ and $\mathbf{MV}^{\bullet+}$ upon reduction of the three BIPY^{2+} dications to $\mathrm{BIPY}^{\bullet+}$ radical cation in solution. Typically, the first reduction potential of the BIPY^{2+} units is shifted[4a] to more positive potentials on account of the presence of favorable radical-pairing interactions. Cyclic voltammetry (CV) and differential pulse voltammetry (DPV) experiments, however, have demonstrated (see the SI) that the first reduction potentials in the equimolar mixture of $\mathbf{C}^{4+}$ and $\mathbf{MV}^{2+}$ remain the same as the individual components alone in MeCN solution. The formation of an inclusion complex has also been investigated by UV/vis spectroscopy using both electrochemical reduction at −0.600 V (vs Ag/AgCl) or chemical reduction[11] by zinc dust. The UV/vis spectra under reductive conditions produced an absorption band, which is associated with the monomeric $\mathrm{BIPY}^{\bullet+}$ radical cation, centered at 610 nm. The characteristic[12] NIR absorption band for the $(\mathrm{BIPY}^{\bullet+})_2$ radical dimer was only observed (see the SI) at relatively high concentrations. These results suggest that the association between $\mathbf{C}^{2(\bullet+)}$ and $\mathbf{MV}^{\bullet+}$ is quite a weak one in solution. Despite the weak association in solution,[13] we were able to grow single crystals from a mixture of $\mathbf{C}\cdot 4\mathrm{PF}_6$ and $\mathbf{MV}\cdot 2\mathrm{PF}_6$ in MeCN after reduction with zinc dust in a glovebox and slow evaporation of $i\mathrm{Pr}_2\mathrm{O}$ into the MeCN solution after removal of the zinc dust. The solid-state superstructure[14] (Figure 1a) reveals (i) the presence of a 1:1 complex with $5\mathrm{PF}_6^-$ ions with (ii) the docking of methyl viologen inside the cavity of the [2]catenane in state **II**. The presence of *five* counterions points to a monoradical state for the overall complex $[(\mathbf{MV}{\subset}\mathbf{C})^{(\bullet+)(4+)}]$ even although the initial solution was comprised[15] of a mixture of $\mathbf{MV}^{\bullet+}$ and $\mathbf{C}^{2(\bullet+)}$. The 1:1 complex is stabilized (Figure 1b,c) by $\pi\cdots\pi$ stacking and C–H···O interactions[16] between the oxygens in the polyether loops and the α-hydrogens on the bipyridinium units. Close contacts (2.5–2.8 Å) also exist between the oxygens and hydrogens of the methyl groups on the methyl viologen, contributing possibly to the preferential docking in state **II** in the solid state. The $\pi\cdots\pi$ stacking distance between the methyl viologen and the encircled bipyridinium unit of the cyclophane is 3.38 Å, suggesting that the monoradical is either localized on one of these units or delocalized between them. The TTF unit is involved in $\pi\cdots\pi$ stacking interactions (interplanar separation, 3.51 Å) with the alongside bipyridinium unit while the plane-to-plane separation with the methyl viologen is 3.70 Å, reflecting the fact that it is interacting more so with the encircled bipyridinium unit. The DNP unit is also engaged in $\pi\cdots\pi$ interactions with the encircled bipyridinium unit with an interplanar separation of 3.30 Å. The packing (Figure 1e) of the complex relies on the formation of intermolecular $\pi\cdots\pi$ stacking interactions (3.40 Å) between the DNP units and the alongside bipyridinium units of the adjacent [3]pseudorotacatenane. The formation of polar donor–acceptor stacks in the extended structure also indicates that the alongside bipyridinium unit exists in the fully oxidized state (BIPY^{2+}) to maximize the interactions in the solid-state superstructure of the $[(\mathbf{MV}{\subset}\mathbf{C})^{(\bullet+)(4+)}]$ complex.

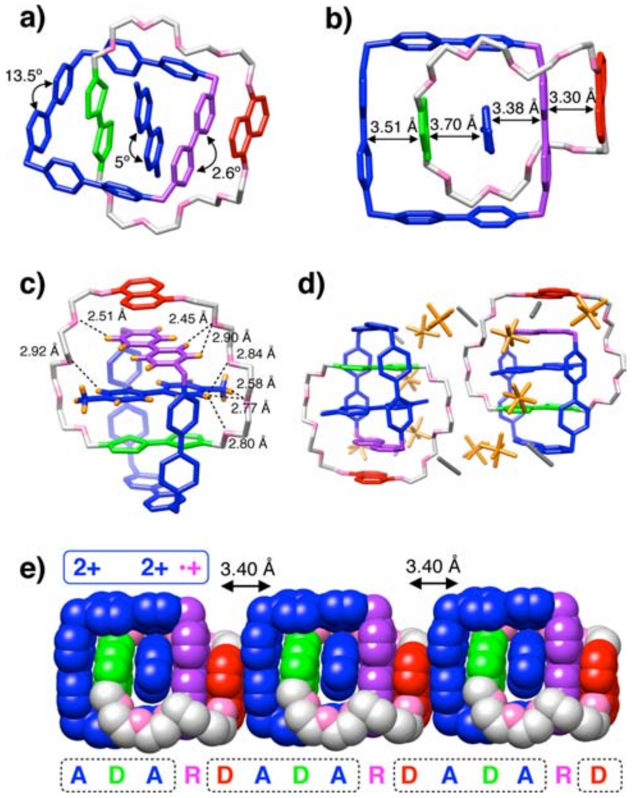

Figure 1. Side-on (a,c) and plan (b) views of tubular representations of the solid-state superstructure of $[(\mathbf{MV}{\subset}\mathbf{C})^{(\bullet+)(4+)}]$ showing (a) the torsional angles around the 4,4′-C–C bond of the bipyridinium units, (b) the π–π stacking distances within the 1:1 complex, and (c) the C–H···O distances (Å) between the oxygen atoms on the polyether loops and the hydrogen atoms (orange) of the guest and the encircled $\mathrm{BIPY}^{\bullet+}$ unit. (d) Tubular representation of the superstructure $[(\mathbf{MV}{\subset}\mathbf{C})^{(\bullet+)(4+)}]$ present in the unit cell, demonstrating the presence of five PF_6^- counterions per complex. (e) The repeating solid-state superstructure in a space-filling format showing the continuous stacks of discrete donor–acceptor domains interrupted by $\mathrm{BIPY}^{\bullet+}$ radical cations.

To establish the existence of the monoradical state in the complex beyond any doubt, we have performed (Figure 2) solid-state electron paramagnetic resonance (EPR) spectroscopy. In the event, we obtained an isotropic EPR spectrum of some single crystals with a g factor of 2.006, in agreement with the reported[17] g value for the $\mathbf{MV}^{\bullet+}$ radical cation; i.e., the complex contains a single $\mathrm{BIPY}^{\bullet+}$ radical cation.[18] The possibility of a trisradical complex, which would be also

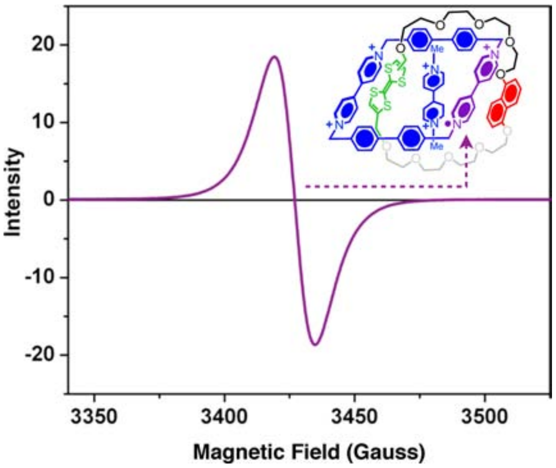

Figure 2. Solid-state EPR spectrum of the single crystals of the [(**MV**⊂**C**)$^{(\bullet+)(4+)}$] complex, demonstrating its monoradical state in accordance with the presence of the five counterions observed by the X-ray crystallography.

expected to be EPR active, can be ruled out by the fact that *five* counterions are associated with the complex.

The assignments of the redox states of the bipyridinium units in the [2]catenane and the bound methyl viologen have been confirmed by analyzing the bond lengths and torsional angles associated with these units in the crystal structure and comparing them with the parameters obtained from the solid-state structure[19] (Figure 3a) of the reduced cyclophane **MS**$^{2(\bullet+)}$. Single crystals were grown in a glovebox by slow vapor diffusion of *i*Pr$_2$O into a solution of **MS**$^{2(\bullet+)}$ in MeCN, generated by reduction of **MS**·4PF$_6$ with zinc dust.[20] The presence of only *two* PF$_6^-$ ions reveals the bisradical nature of the cyclophanes. Its cavity is filled with an *i*Pr$_2$O molecule and the counterions occupy (Figure 3b) the cavities in between the rings. It is well known[5,17a] that the reduction of the BIPY^{2+} dication to a BIPY$^{\bullet+}$ radical cation causes a reduction in the torsional angle around its 4,4′-C−C bond. The increased double-bond character of this bond results in a decrease of its length. The torsional angles of BIPY$^{\bullet+}$ units in the **MS**$^{2(\bullet+)}$ ring are 4.7(6) and 9.0(6)° and the 4,4′-C−C bond lengths in these units have been found to be 1.427(7)and 1.430(7) Å, reflecting their radical cationic nature. The solid-state superstructure (Figure 3c) is comprised of continuous stacks of **MS**$^{2(\bullet+)}$ rings with a centroid-to-centroid separation of 3.30 Å between the BIPY$^{\bullet+}$ units of adjacent **MS**$^{2(\bullet+)}$ rings. The adjacent cyclophanes are also aligned in register with the angle of offset 4.2°.

With all this information to hand, the bond lengths and torsional angles of the 4,4′-C−C bond of the three different bipyridinium units in the [(**MV**⊂**C**)$^{(\bullet+)(4+)}$] complex can be analyzed. The bond lengths for the alongside bipyridinium unit and the methyl viologen are very similar to each other, i.e., 1.499(8) and 1.492(12) Å, respectively, reflecting the dicationic nature (BIPY^{2+} and **MV**$^{2+}$) of these units. These distances are also in good agreement with those present[8] in the crystal structures of **C**·4PF$_6$ and the complex [DNP-(DEG)$_2$⊂**C**·4PF$_6$]. This observation leaves (Figure 1e) the encircled bipyridinium unit in the cyclophane adopting the radical cation state (BIPY$^{\bullet+}$). In fact, the 4,4′-C−C bond length is 1.432(8) Å, consistent with that in the **MS**$^{2(\bullet+)}$ ring as well as in the previously reported[17a] **MV**$^{\bullet+}$ radical cation.

Moreover, the torsional angles of the alongside BIPY^{2+} unit and the **MV**$^{2+}$ dication are 13.5(9) and 5(1)°, respectively, whereas that of the encircled BIPY$^{\bullet+}$ unit is the least [2.6(9)°] of all, providing further evidence for its radical-cationic nature. Presumably, the bound **MV**$^{2+}$ in its dicationic form and its preference to reside in the cavity of the [2]catenane in its state **II** geometry increases the overall stability of the complex in the solid state by maximizing the donor−acceptor interactions with the surrounding π-donating TTF unit and also by undergoing dimerization with the BIPY$^{\bullet+}$ unit—a situation which would not be possible if the [2]catenane adopted the state **I** geometry.[21]

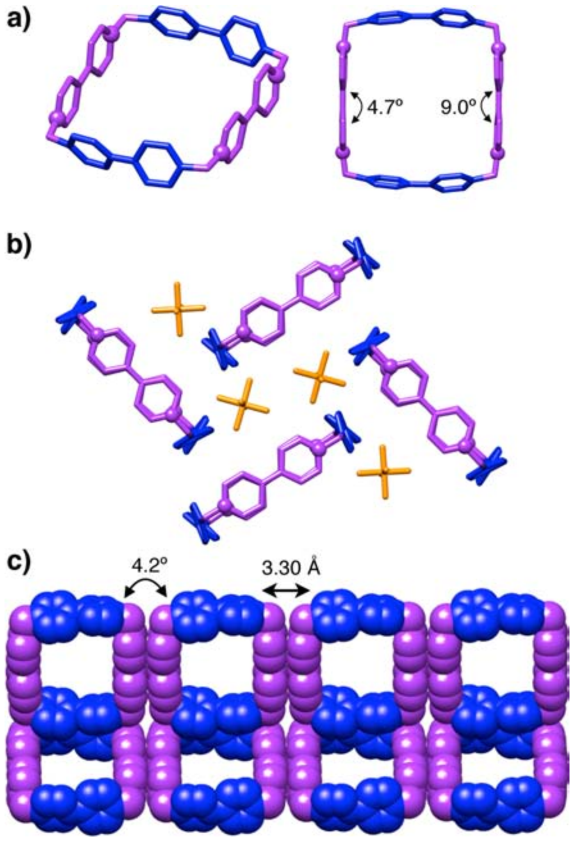

Figure 3. (a) Different views of the solid-state superstructure of **MS**$^{2(\bullet+)}$ ring in tubular representation. Nitrogen atoms are depicted as spheres to differentiate the BIPY$^{\bullet+}$ edges (purple) from the biphenylene edges (blue) of the ring. The counterions and *i*Pr$_2$O molecules occupying the cavity of the ring are not shown for the sake of clarity. (b) View of the unit cell of the **MS**$^{2(\bullet+)}$ ring looking along the crystallographic *c* axis revealing the positions of the PF$_6^-$ counterions all represented by tubes. (c) Space-filling representation of the solid-state packing of **MS**$^{2(\bullet+)}$ rings in one dimension, demonstrating the interactions between their BIPY$^{\bullet+}$ components.

In summary, we have observed the juxtaposition of BIPY^{2+} dications and BIPY$^{\bullet+}$ radical cations in the solid state in a confined environment in which they are surrounded by π-donating units. We have shown that two different binding pockets in a [2]catenane host can be activated selectively by redox chemistry and closed down by a "co-factor", i.e., a guest. This phenomenon is reminiscent[22] of proteins which undergo structural changes in particular circumstances to interact with different substrates as a result of conformational changes within the protein domains.

■ ASSOCIATED CONTENT

Ⓢ Supporting Information

Synthesis and detailed spectroscopic and crystallographic data. This material is available free of charge via the Internet at http://pubs.acs.org.

■ AUTHOR INFORMATION

Corresponding Author

stoddart@northwestern.edu

Author Contributions

‡G.B. and M.F. contributed equally.

Notes

The authors declare no competing financial interest.

■ ACKNOWLEDGMENTS

G.B., M.F., and J.F.S. are supported by the Non-Equilibrium Energy Research Center which is an Energy Frontier Research Center (EFRC) funded by the U.S. Department of Energy, Offices of Basic Energy Sciences (DOE-BES), under Award DE-SC0000989. M.R.W. and S.M.D. are supported by the U.S. National Science Foundation under Grant No. CHE-1012378. R.C. is supported by the Argonne-Northwestern Solar Energy Research (ANSER) Center, which is an EFRC funded by the DOE-BES under Award DE-SC0001059 (EPR Spectroscopy).

■ REFERENCES

(1) (a) Schill, G. *Catenanes, Rotaxanes and Knots*; Academic Press: New York, 1971. (b) Dietrich-Buchecker, C. O.; Sauvage, J.-P. *Catenanes, Rotaxanes, and Knots—A Journey Through the World of Molecular Topology*; Wiley-VCH: Weinheim, 1999. (c) Stoddart, J. F. *Chem. Soc. Rev.* **2009**, *38*, 1802.

(2) (a) Busch, D. H.; Stephenson, N. A. *Coord. Chem. Rev.* **1990**, *100*, 119. (b) Anderson, S.; Anderson, H. L.; Sanders, J. K. M. *Acc. Chem. Res.* **1993**, *26*, 469. (c) Hubin, T. J.; Busch, D. H. *Coord. Chem. Rev.* **2000**, *200*, 5. (d) Blanco, M.-J.; Chambron, J.-C.; Jimenez, M.-C.; Sauvage, J.-P. *Top. Stereochem.* **2003**, *23*, 125. (e) Schalley, C. A.; Weilandt, T.; Bruggemann, J.; Vögtle, F. *Top. Curr. Chem.* **2004**, *248*, 141. (f) Aricó, F.; Badjić, J. D.; Cantrill, S. J.; Flood, A. H.; Leung, K. C.-F.; Liu, Y.; Stoddart, J. F. *Top. Curr. Chem.* **2005**, *249*, 203. (g) Vickers, M. S.; Beer, P. D. *Chem. Soc. Rev.* **2007**, *36*, 211. (h) Qu, D. H.; Tian, H. *Chem. Sci.* **2011**, *2*, 1011.

(3) Barin, G.; Coskun, A.; Fouda, M. M. G.; Stoddart, J. F. *ChemPlusChem* **2012**, *77*, 159.

(4) (a) Trabolsi, A.; Khashab, N.; Fahrenbach, A. C.; Friedman, D. C.; Colvin, M. T.; Cotí, K. K.; Benítez, D.; Tkatchouk, E.; Olsen, J.-C.; Belowich, M. E.; Carmielli, R.; Khatib, H. A.; Goddard, W. A., III; Wasielewski, M. R.; Stoddart, J. F. *Nat. Chem.* **2010**, *2*, 42. (b) Li, H.; Fahrenbach, A. C.; Dey, S. K.; Basu, S.; Trabolsi, A.; Zhu, Z.; Botros, Y. Y.; Stoddart, J. F. *Angew. Chem., Int. Ed.* **2010**, *49*, 8260.

(5) Fahrenbach, A. C.; Barnes, J. C.; Lanfranchi, D. A.; Li, H.; Coskun, A.; Gassensmith, J. J.; Liu, Z. C.; Benítez, D.; Trabolsi, A.; Goddard, W. A.; Elhabiri, M.; Stoddart, J. F. *J. Am. Chem. Soc.* **2012**, *134*, 3061.

(6) (a) Li, H.; Fahrenbach, A. C.; Coskun, A.; Zhu, Z. X.; Barin, G.; Zhao, Y. L.; Botros, Y. Y.; Sauvage, J.-P.; Stoddart, J. F. *Angew. Chem., Int. Ed.* **2011**, *50*, 6782. (b) Barnes, J. C.; Fahrenbach, A. C.; Dyar, S. M.; Frasconi, M.; Giesener, M. A.; Zhu, Z. X.; Liu, Z. C.; Hartlieb, K. J.; Carmieli, R.; Wasielewski, M. R.; Stoddart, J. F. *Proc. Natl. Acad. Sci. U.S.A.* **2012**, *109*, 11546. (c) Zhu, Z. X.; Fahrenbach, A. C.; Li, H.; Barnes, J. C.; Liu, Z. C.; Dyar, S. M.; Zhang, H. C.; Lei, J. Y.; Carmieli, R.; Sarjeant, A. A.; Stern, C. L.; Wasielewski, M. R.; Stoddart, J. F. *J. Am. Chem. Soc.* **2012**, *134*, 11709. (d) Fahrenbach, A. C.; Zhu, Z. X.; Cao, D.; Liu, W. G.; Li, H.; Dey, S. K.; Basu, S.; Trabolsi, A.; Botros, Y. Y.; Goddard, W. A.; Stoddart, J. F. *J. Am. Chem. Soc.* **2012**, *134*, 16275.

(7) Fahrenbach, A. C.; Sampath, S.; Late, D. J.; Barnes, J. C.; Kleinman, S. L.; Valley, N.; Hartlieb, K. J.; Liu, Z.; Dravid, V. P.; Schatz, G. C.; Van Duyne, R. P.; Stoddart, J. F. *ACS Nano* **2012**, *6*, 9964.

(8) Barin, G.; Coskun, A.; Friedman, D. C.; Olson, M. A.; Colvin, M. T.; Carmielli, R.; Dey, S. K.; Bozdemir, O. A.; Wasielewski, M. R.; Stoddart, J. F. *Chem.—Eur. J.* **2011**, *17*, 213.

(9) Amabilino, D. B.; Ashton, P. R.; Bravo, J. A.; Raymo, F. M.; Stoddart, J. F.; White, A. J. P.; Williams, D. J. *Eur. J. Org. Chem.* **1999**, 1295.

(10) The [3]rotacatenane has also allowed us to investigate TTF radical dimer formation. See ref 8. Cf.: Coskun, A.; Spruell, J. M.; Barin, G.; Fahrenbach, A. C.; Forgan, R. S.; Colvin, M. T.; Carmieli, R.; Benítez, D.; Tkatchouk, E.; Friedman, D. C.; Sarjeant, A. A.; Wasielewski, M. R.; Goddard, W. A., III; Stoddart, J. F. *J. Am. Chem. Soc.* **2011**, *133*, 4538.

(11) Endo, T.; Ageishi, K.; Okawara, M. *J. Org. Chem.* **1986**, *51*, 4309.

(12) (a) Kosower, E. M.; Cotter, J. L. *J. Am. Chem. Soc.* **1964**, *86*, 5524. (b) Jeon, W. S.; Ziganshina, A. Y.; Lee, J. W.; Ko, Y. H.; Kang, J.-K.; Lee, C.; Kim, K. *Angew. Chem., Int. Ed.* **2003**, *42*, 4097. (c) Trabolsi, A.; Hmadeh, M.; Khashab, N. M.; Friedman, D. C.; Belowich, M. E.; Humbert, N.; Elhabiri, M.; Khatib, H. A.; Albrecht-Gary, A. M.; Stoddart, J. F. *New J. Chem.* **2009**, *33*, 254.

(13) For literature examples regarding the crystallization of complexes that are weakly associated in solution, see: Northrop, B. H.; Khan, S. J.; Stoddart, J. F. *Org. Lett.* **2006**, *8*, 2159. Forgan, R. S.; Gassensmith, J. J.; Cordes, D. B.; Boyle, M. M.; Hartlieb, K. J.; Friedman, D. C.; Slawin, A. M. Z.; Stoddart, J. F. *J. Am. Chem. Soc.* **2012**, *134*, 17007.

(14) Crystal data for $[(\mathbf{MV}\subset\mathbf{C})^{(\bullet+)(4+)}]\cdot5PF_6$: $(C_{94}H_{98}N_6O_{10}S_4)$ $5(PF_6)$ $2.69(C_2H_3N)$, $M = 2435.27$, triclinic, space group $P1$ (no. 2), $a = 12.4129(4)$, $b = 17.3342(6)$, $c = 26.3774(8)$ Å, $\alpha = 90.882(2)$, $\beta = 95.194(2)$, $\gamma = 90.489(2)°$, $V = 5651.3(3)$ Å^3, $T = 100.0$ K, $Z = 2$, $\rho_{calc} = 1.431$ g cm^{-3}, $\mu(CuK\alpha) = 2.398$ mm^{-1}. 19357 reflections measured, 19357 unique ($R_{int} = 0.0508$) which were used in all calculations. $R_1(F^2 > \sigma F^2) = 0.1210$, $wR_2 = 0.3627$. CCDC 917010.

(15) We have observed (see ref 6d) a similar situation during the crystallization of a [2]catenane in which the bisradical state was obtained despite the fact that a trisradical is present in solution initially.

(16) (a) Houk, K. N.; Menzer, S.; Newton, S. P.; Raymo, F. M.; Stoddart, J. F.; Williams, D. J. *J. Am. Chem. Soc.* **1999**, *121*, 1479. (b) Raymo, F. M.; Bartberger, M. D.; Houk, K. N.; Stoddart, J. F. *J. Am. Chem. Soc.* **2001**, *123*, 9264.

(17) (a) Bockman, T. M.; Kochi, J. K. *J. Org. Chem.* **1990**, *55*, 4127. (b) Yoon, K. B.; Kochi, J. K. *J. Am. Chem. Soc.* **1988**, *110*, 6586.

(18) After dissolving the crystals from the EPR measurements in MeCN and allowing them to be oxidized in air, we recorded the ^1H NMR spectrum (see the SI), which shows a 1:1 ratio of $\mathbf{MV}^{2+}$ and $\mathbf{C}^{4+}$, confirming that the observed EPR activity results from the crystals of the $[(\mathbf{MV}\subset\mathbf{C})^{(\bullet+)(4+)}]$ complex.

(19) Crystal data for $\mathbf{MS}^{2(\bullet+)}\cdot2PF_6$: $(C_{48}H_{40}N_4)$ $2(PF_6)$ $0.8(C_6H_{14}O)$, $M = 1044.52$, orthorhombic, space group $P2_12_12$ (no. 18), $a = 19.0012(6)$, $b = 11.2967(4)$, $c = 13.7427(5)$ Å, $V = 2949.88(18)$ Å^3, $T = 100.01$ K, $Z = 2$, $\rho_{calc} = 1.176$ g cm^{-3}, $\mu(CuK\alpha) = 1.319$ mm^{-1}. 16360 reflections measured, 4814 unique ($R_{int} = 0.1184$) which were used in all calculations. $R_1(F^2 > \sigma F^2) = 0.0530$, $wR_2 = 0.1193$. CCDC 916870.

(20) It should be noted that when the crystallization is carried out in the presence of $\mathbf{MV}^{\bullet+}$, we obtain single crystals of $\mathbf{MS}^{2(\bullet+)}$ without fail.

(21) We have also observed close C−H···F contacts (see the SI) between the encircled $BIPY^{\bullet+}$ and $\mathbf{MV}^{2+}$ units and the surrounding PF_6^- counterions, which could be contributing to the stabilization of these species since they are in close proximity.

(22) (a) Lindsley, J. E.; Rutter, J. *Proc. Natl. Acad. Sci. U.S.A.* **2006**, *103*, 10533. (b) Goodey, N. M.; Benkovic, S. J. *Nat. Chem. Biol.* **2008**, *4*, 474.